Eur. Phys. J. D **4**, 189–197 (1998)

THE EUROPEAN PHYSICAL JOURNAL D

Resonance enhanced multiphoton ionization (REMPI) and REMPI-photoelectron spectroscopy of ammonia

M.N.R. Ashfold[1], S.R. Langford[1], R.A. Morgan[1], A.J. Orr-Ewing[1], C.M. Western[1], C.R. Scheper[2], and C.A. de Lange[2,a]

[1] School of Chemistry, University of Bristol, Bristol BS8 1TS, UK
[2] Laboratory for Physical Chemistry, University of Amsterdam, Nieuwe Achtergracht 127, 1018 WS Amsterdam, The Netherlands

Received: 28 January 1998 / Revised: 3 April 1998 / Accepted: 15 April 1998

Abstract. Resonance enhanced multiphoton ionization (REMPI) spectroscopy, preferably linked with kinetic energy analysis of the resulting photoelectrons (REMPI-photoelectron spectroscopy (PES)), continues to make enormous contributions to our understanding of the spectroscopy and, in many cases, the decay dynamics of small molecules in excited (normally Rydberg) electronic states. Here we present results of recent REMPI and REMPI-PES studies involving the ammonia molecule which provide further illustration of some of the many opportunities offered by these techniques.

PACS. 33.60.-q Photoelectron spectra – 33.80.Rv Multiphoton ionization and excitation to highly excited states (e.g., Rydberg states) – 34.50.Gb Electronic excitation and ionization of molecules; intermediate molecular states (including lifetimes, state mixing, etc.)

1 Introduction

Resonance enhanced multiphoton ionization (REMPI) spectroscopy is now well-established as a valuable method for investigating the structure and, in favorable cases, the decay dynamics of many of the more long lived excited electronic states (most notably Rydberg states) of small and medium sized gas phase molecules [1]. Additional information (for example, structural data for the resulting ions and/or insight into molecular photoionization dynamics) can be obtained when the REMPI method is combined with kinetic energy (KE) analysis of the accompanying photoelectrons – a technique normally identified with the name REMPI-photoelectron spectroscopy (PES). The present work highlights recent REMPI and REMPI-PES investigations of the ammonia molecule as a means of illustrating many of these strengths [2]. Ammonia has a pyramidal (C_{3v}) equilibrium geometry in its ground state, with an electronic configuration most usually written as:

$$(1a_1')^2(2a_1')^2(1e')^4(1a_2'')^2;\ \tilde{X}^1A_1'. \qquad (1)$$

Excited states arising as a result of electronic promotion from the highest occupied $1a_2''$ *lone pair* molecular orbital all have planar (D_{3h}) equilibrium geometries. This, and the modest size of the potential barrier to inversion in the ground state, justifies description (as above) of the *ground* state configuration in terms of D_{3h} symmetry labels.

The excited electronic states of ammonia have been the subject of many previous experimental and theoretical studies, addressing their spectroscopy, their complex predissociation pathways and, in some cases, their detailed photochemistry. Much of the earlier spectroscopic work involved conventional ultraviolet (UV) and, particularly, vacuum ultraviolet (VUV) gas phase absorption measurements of the vertical electronic spectrum [3–6]. The congested nature of these spectra, however, precluded many definitive assignments. The congestion arises, in part, because each electronic transition appears in the form of a long vibronic progression associated with excitation of the out-of-plane mode ν_2' (an inevitable consequence of the Franck-Condon principle and the planar ← pyramidal geometry change that results upon electronic promotion from the $1a_2''$ orbital), but is compounded by the spectral line broadening due to predissociation of many of these excited states. Our current level of understanding is to a large extent a result of the introduction of REMPI spectroscopy, allied with jet-cooling techniques, and the seminal work of Colson *et al.* [7,8]. They recorded and compared the three-photon REMPI spectra and the VUV absorption spectra of both NH_3 and ND_3 over the wavenumber range $\sim$ 62 500–80 000 cm^{-1} and provided what, at the time, was the most complete global description of the electronic spectrum of ammonia. Much of the subsequent work has been concerned with extending and refining parts of this spectroscopic analysis and/or with

[a] e-mail: delange@fys.chem.uva.nl

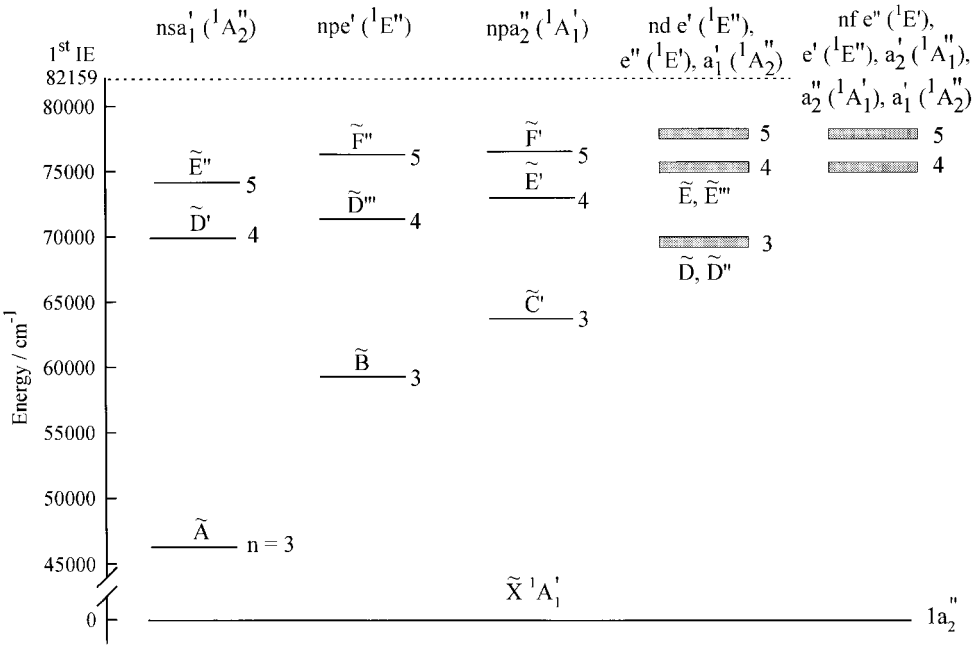

Fig. 1. Diagram showing observed and/or predicted members (with $n \leq 5$) of the first few Rydberg series of ammonia. State labels (following Refs. [2,8]) and symmetries are shown, along with the appropriate value of the principal quantum number, n.

detailed analysis of the predissociation mechanisms affecting some of the lower lying Rydberg states.

The small size and high symmetry of ammonia has encouraged description of its molecular orbitals within the framework of an appropriate united atom (neon), split by a field of D_{3h} symmetry. All documented excited electronic states fit within such a model, involving electron promotion to an orbital with principal quantum number $n \geq 3$; all are thus regarded as Rydberg states. Figure 1 illustrates the lowest energy part of the pattern of states predicted by this model. For clarity, only states derived from orbitals with $n \leq 5$ and $\ell \leq 3$ are shown; Rydberg states involving orbitals with higher n should exhibit the same energetic pattern, whilst states derived from higher ℓ functions are not considered further because of their presumed inaccessibility *via* a two-photon excitation (such as considered here) from an initial orbital possessing hybrid s/p character [1].

The spectroscopy and photochemistry of the first excited $\tilde{A}^1A_2''$ ($3sa_1' \leftarrow 1a_2''$) state of ammonia has been the subject of much attention. The 298 K $NH_3(\tilde{A}-\tilde{X})$ absorption spectrum shows vibrational (a progression in ν_2') but no rotational fine structure; the 0_0^0 and 2_0^1 bands of the corresponding system in ND_3 do exhibit some resolvable rotational structure [4]. Our present understanding of this efficient predissociation process ($k_{predissociation} \sim 10^{12}-10^{13}$ s^{-1}) derives from a number of sources: rotational state lifetimes and decay rates deduced from simulation of individual $\tilde{A} \leftarrow \tilde{X}$ vibronic band contours [9,10] and from direct linewidth measurements of fully resolved rovibronic transitions revealed by double resonance methods, *e.g.* by stimulated emission pumping (SEP) following multiphoton preparation of $\tilde{C}'$ state molecules [10,11] or in microwave-optical double resonance experiments [12]; *ab initio* calculations of the $\tilde{A}$ state potential energy surface [13]; and measurements and modeling of the energy disposal [14,15] and the recoil velocity and angular momentum vector correlations [16,17] in the NH_2 photofragments. Taken together, these studies now afford a remarkably detailed picture of the photofragmentation dynamics of $\tilde{A}$ state ammonia molecules, which have been summarized elsewhere [18,19] and will not be discussed further.

The $3pe' \leftarrow 1a_2''$ and $3pa_2'' \leftarrow 1a_2''$ electronic promotions give rise to the $\tilde{B}^1E''-\tilde{X}^1A_1'$ and $\tilde{C}'^1A_1'-\tilde{X}^1A_1'$ systems, respectively. Members of the 2_0^n vibronic progression associated with the former transition have been identified, in both NH_3 and ND_3, *via* VUV absorption spectroscopy [3,20,21], but our detailed understanding of the $\tilde{B}$ state has been much enhanced by two-photon REMPI spectroscopy studies both under beam conditions [22] and, with sub-Doppler resolution, in the bulk [23]. Several rotationally resolved double resonance studies, in which $\tilde{B}$ state levels associated with excitation of one quantum of each of the doubly degenerate vibrations ν_3' and ν_4' (built on a progression in ν_2') were populated following initial excitation of molecules into selected rovibrational levels of the $\tilde{X}$ [24–26] or $\tilde{A}$ [27,28] states have helped clarify the extent of Jahn-Teller distortion affecting the $\tilde{B}^1E''$ state and prove that the historically labeled $\tilde{C}-\tilde{X}$ system of ammonia actually involves a vibronic component of the $\tilde{B}$ state. The $\tilde{C}'^1A_1'-\tilde{X}^1A_1'$ system has negligible oscillator strength in the one-photon spectrum but shows as a well-resolved progression (in ν_2'), interspersed among the various $\tilde{B}-\tilde{X}$ features, in both two and three-photon REMPI [7,29,30]. Double resonant multiphoton excitation, *via* the $\tilde{A}$ state,

has provided one route to identifying the $\tilde{C}'$ state symmetric stretching mode (ν_1') in both NH_3 and ND_3 [27]. The former was also identified in one of the first REMPI-PES studies of jet-cooled NH_3 molecules [31]. Picosecond pump-probe REMPI-PES studies have allowed real time observation of the decay of selected vibronic levels of both the $\tilde{B}$ and $\tilde{C}'$ states [32].

Progressing to higher energies, the spectrum of ammonia becomes ever more complex, reflecting the increased electronic state density (see Fig. 1) and the consequent increase in Franck-Condon accessible vibronic levels as we approach the first ionization limit (IE = 82 159 cm^{-1} in the case of NH_3 [33]). The availability of rotationally "cold" spectra, obtained using jet-cooled samples, has been essential in unravelling a significant part of this congested level structure. Li and Vidal [21] identified a 2_0^n vibronic progression in the VUV excitation spectrum of both NH_3 and ND_3 by monitoring either fluorescence from the fraction of NH_2 (ND_2) photofragments that are formed in their excited $\tilde{A}^2A_1$ state or parent ions that result from absorption of a visible photon by the VUV prepared state (*i.e.* 1+1' two color REMPI); rotational analysis shows that this progression must be associated with the $\tilde{D}^1E'-\tilde{X}^1A_1'$ ($3de'' \leftarrow 1a_2''$) transition. Parallel analyses of VUV absorption spectra and/or 3+1 REMPI spectroscopy [8] indicate that another member of the $3d \leftarrow 1a_2''$ complex (the $\tilde{D}''^1A_2''-\tilde{X}$ transition, associated with the orbital promotion $3da_1' \leftarrow 1a_2''$), has its electronic origin in the same energy region, as do the $\tilde{D}'^1A_2''-\tilde{X}$ ($4sa_1' \leftarrow 1a_2''$) and $\tilde{D}'''^1E''-\tilde{X}$ ($4pe' \leftarrow 1a_2''$) transitions. Energetic considerations dictate that the "missing" $^1E''(3de' \leftarrow 1a_2'')$ excited state must also lie in this energy range but it remains to be identified. The situation at still higher energies becomes ever less complete. Virtually all recent progress [2,34] has come from 2 + 1 REMPI spectroscopy, much of it in conjunction with REMPI-PES studies similar to those reported here. In the remainder of this paper we will concentrate on a number of illustrative examples involving the ammonia molecule which serve to demonstrate various of the merits (and some of the remaining limitations) of the REMPI and REMPI-PES techniques.

2 Experimental

Results described herein were obtained using two complementary experimental set-ups: in Bristol, a home-built time-of-flight (TOF) mass spectrometer was used to record *mass* resolved REMPI spectra of jet-cooled NH_3 and ND_3 molecules and fragments arising from their photodissociation, whilst in Amsterdam REMPI-PES studies were performed using a "magnetic bottle" spectrometer. Both experiments have been described previously [2,35] and thus only brief descriptions of the apparatus and procedures are presented here.

REMPI spectra were recorded in Bristol using a pulsed nozzle to introduce NH_3 or ND_3 (5% mix seeded in ~ 1 atm Ar) into the source region of a home-built TOF mass spectrometer. The gas pulses were crossed by the focused (*f.l.* 30–50 cm) frequency doubled output of a tunable Nd:YAG pumped dye laser. Ions formed by REMPI in the source region were subjected to two stages of acceleration prior to entering a field-free drift region and were detected by a pair of chevron-configuration microchannel plates. The resulting signal was accumulated by a digital oscilloscope and downloaded to a computer *via* a GPIB interface for subsequent analysis. To obtain mass selected REMPI spectra, the dye laser was scanned and only that part of the total ion signal that fell within a narrow time window centered on the TOF of the mass of interest was collected, averaged, and stored. Wavelength calibration (in the visible spectral region) was achieved by recording the optogalvanic spectrum of neon excited in a hollow cathode discharge simultaneously with the REMPI spectrum of interest.

REMPI-PE spectra were obtained in Amsterdam using an XeCl excimer pumped dye laser system with the laser output focused (*f.l.* = 2.5 cm) into the ionization region of a magnetic bottle photoelectron spectrometer. These experiments employed an effusive beam of pure NH_3 or ND_3 vapor. This was intercepted at right angles by the focused laser beam, and photoelectrons resulting from each laser pulse were extracted along the third orthogonal axis into the spectrometer. The measured times of arrival of the photoelectrons at a pair of MCPs situated at the end of the 50 cm flight tube were used to determine electron kinetic energies. A transient digitizer, interfaced to a PC, recorded pre-amplified output signals from the microchannel plates. Kinetic-energy-resolved photoelectron spectra were obtained by progressively stepping the retarding voltage on a grid in the flight tube and, at each voltage setting, performing a time-to-energy transformation on just the slowest (*i.e.* highest resolution) part of the TOF spectrum, with a resultant 15 meV (FWHM) resolution at all kinetic energies in the present experiments. To place the photoelectron kinetic energies on an absolute scale, the ammonia sample was doped with xenon and well-documented REMPI transitions terminating on the two spin-orbit states of the Xe^+ ion were then used to calibrate the REMPI-PE spectra. Some wavelength-resolved REMPI spectra were also recorded in Amsterdam by measuring both the total and selected energy portions of the photoelectron yield as a function of excitation wavelength.

3 Results and discussion

Figure 2a shows a mass resolved 2+1 REMPI spectrum of jet-cooled ND_3 (monitoring just parent ions with m/z 20) recorded using linearly polarized laser radiation at wavelengths ~ 292 nm. Given previous analyses [3,21–23] of lower 2_0^n members of the $\tilde{B}-\tilde{X}$ two-photon transition in NH_3 and ND_3, and the fact that the $\tilde{B}-\tilde{X}$ electronic promotion is known to be carried exclusively by the $T_1^2(A)$ component of the two-photon transition tensor [22,23], it is a relatively straightforward exercise to show that this particular spectrum involves a $^1E''-^1A_1'$ vibronic transition, originating from the lower (0^+) inversion level of the

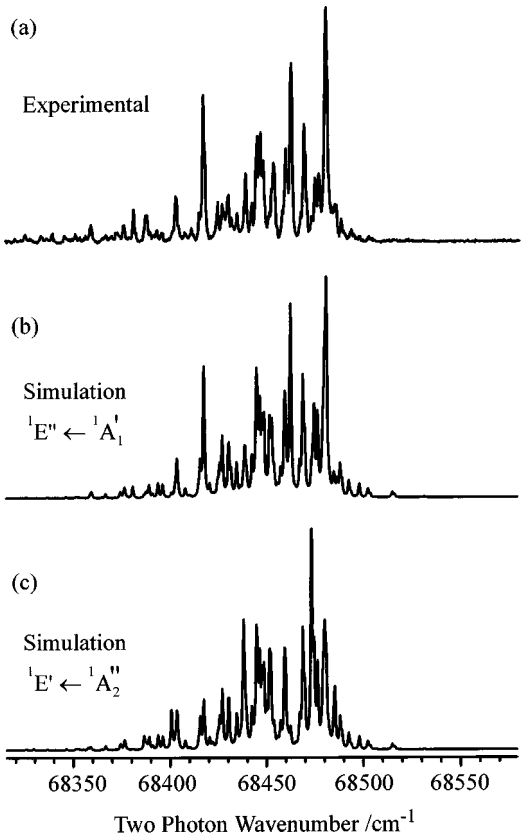

Fig. 2. (a) 2 + 1 REMPI spectrum of ND_3 obtained using linearly polarized laser radiation and monitoring the yield of ions with m/z 20, as a function of wavelength over the range 292.68–291.55 nm ($2\bar{\nu}$ = 68 315–68 580 cm^{-1}). (b) Simulated two-photon excitation spectrum of this $\tilde{B}-\tilde{X}$ 2_0^{12} band obtained using literature values (Ref. [39]) for the ground state constants, the following excited state parameters: ν_0 = 68 446.20(3) cm^{-1}, B = 3.526(5) cm^{-1}, C = 2.84(1) cm^{-1}, ξ = 0.784(6) and fixing q_v and the distortion constants to 0 – determined by least squares fitting in terms of the appropriate symmetric top Hamiltonian (Ref. [22]), a transition linewidth of 0.9(1) cm^{-1} (assumed Gaussian and largely determined by the laser bandwidth), a rotational temperature of 40 K, and assuming the transition to be carried solely by the $T_1^2(A)$ component of the two-photon transition tensor; (c) shows the corresponding simulation that results if we use the *same* spectroscopic constants but assume the spectrum to be due to a $^1E'-{}^1A_2''$ vibronic transition (as would be the case if the resonance enhancing $\tilde{B}$ state level had odd v_2' quantum number and the transition thus originated from the 0^- level of the ground state).

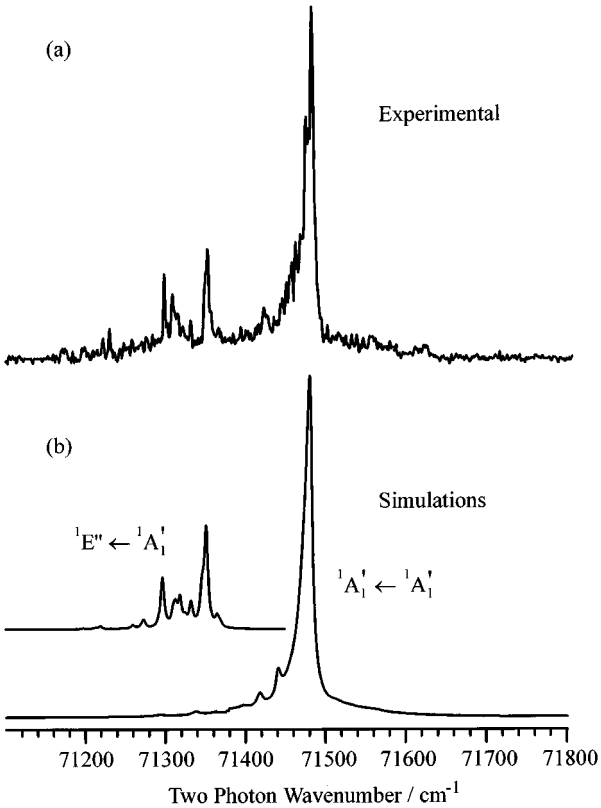

Fig. 3. (a) 2 + 1 REMPI spectrum of jet-cooled NH_3 recorded using linearly polarized laser radiation and monitoring just those ions with TOF appropriate to m/z 17, over the wavelength range 281.21–278.47 nm ($2\bar{\nu}$ = 71 100–71 800 cm^{-1}). (b) Approximate simulations showing the relative extents of the two overlapping $\tilde{C}'-\tilde{X}$ 2_0^8 and $\tilde{B}-\tilde{X}$ 2_0^{12} band contours (see text for further details).

ground state. Thus we can conclude that the 2^n level resonant at the two-photon energy involves an *even* number of out of plane bending quanta; the band origin and rotational constants returned in the best-fit simulation of the spectrum (Fig. 2b) are consistent with assignment in terms of 2 + 1 REMPI *via* the $\tilde{B}$, $v_2' = 12$ state. Figure 2c shows a simulated two-photon spectrum using the same spectroscopic constants for the lower and upper states, but assuming the spectrum to arise as a result of a $^1E'-{}^1A_2''$ vibronic transition (as would be the case if the resonance enhancing $\tilde{B}$ state level had *odd* v_2' quantum number and the transition thus originated from the 0^- inversion component of the ground state). This provides a much inferior reproduction of the relative line intensities appearing in the experimental spectrum (reflecting the different nuclear spin statistics associated with the J'' levels contributing to the $K'' = 0$ sub-bands that originate from $^1A_1'(0^+)$ and $^1A_2''(0^-)$ vibronic states [21]) and serves to highlight the level of detail and accuracy achievable with the "traditional" methods of molecular spectroscopy in cases where it is possible to observe and analyze the rotational fine structure associated with an isolated vibronic transition.

Turning now to consider the corresponding $\tilde{B}-\tilde{X}$ 2_0^{12} band in the 2 + 1 REMPI spectrum of NH_3 we begin to see some of the potential problems from spectral overlap, even in jet-cooled spectroscopy. As Figure 3 shows, the $\tilde{B}-\tilde{X}$ 2_0^{12} band falls on the low wavenumber side of a more intense feature. Given the simplification afforded by jet-cooling and knowledge of the pattern of vibronic structure appearing at lower wavenumber [2,8, 21], interpretation of this spectral region presents no real difficulty: the more intense feature can be assigned to

the $\tilde{C}'-\tilde{X}$ 2_0^8 band. Both this assignment, and that of the $\tilde{B}-\tilde{X}$ 2_0^{12} band, can be confirmed by REMPI-PES measurements of the kind described below. The accompanying band contour simulations are, of necessity, somewhat approximate since both excited states are predissociated [29,30] to the extent that lifetime broadening precludes resolution of individual lines. Ground state spectroscopic parameters used in their construction were taken from Urban *et al.* [36], whilst excited state parameters used were as follows: $\tilde{B}-\tilde{X}$ 2_0^{12}: $\nu_0 = 71\,315(1)$ cm^{-1}, $B' = 5.43(6)$ cm^{-1}, $C' = 5.9(1)$ cm^{-1}, $\zeta = 0.58(6)$, with q_v and the centrifugal distortion constants fixed at 0, and a transition linewidth $\omega = 5.7(3)$ cm^{-1} (assumed Lorentzian, and largely determined by the short excited state lifetime); $\tilde{C}'-\tilde{X}$ 2_0^8: $\nu_0 = 71\,483(2)$ cm^{-1}, $B = 8.1(2)$ cm^{-1}, $C = 5.7(3)$ cm^{-1}. The best-fit rotational temperature in each case was $T_{rot} = 40$ K. The $\tilde{C}'-\tilde{X}$ 2_0^8 band contour simulation assumes contributions from both the $T_0^0(A)$ and $T_0^2(A)$ components of the two-photon transition tensor (relative amplitudes 1.0:0.8) and that the $\tilde{C}'$ 2^8 excited state lifetime shows a rotational level dependence whereby the transition linewidths (assumed Lorentzian) vary according to the relationship [2,22,37]:

$$\omega_{J'K'} = \omega_0\Big\{1 + a[J'(J'+1) + bK'^2]\Big\}, \qquad (2)$$

with $\omega_0 = 3.9(2)$ cm^{-1}, $a = 0.7(2)$ and $b = -1$.

Spectral congestion and blending, in many cases exacerbated by lifetime broadening, become ever more problematic at higher energies. By way of illustration, consider the portion of the jet-cooled NH_3 REMPI spectrum shown in Figure 4 and, in particular, the features at $2\tilde{\nu} \sim 78\,140$ cm^{-1} and $\sim 78\,495$ cm^{-1} (shown on an expanded scale in the two insets). REMPI-PES holds the key to definitive assignment in such situations. The Rydberg state (or states) of interest typically have the same core configuration as the ionic state that lies at the convergence limit of the series to which they belong (*i.e.* that of the ground state ion in this case). Thus the final $NH_3^+ \leftarrow NH_3$(Rydberg) ionizing transition(s) will be between states having very similar equilibrium geometries. In such cases, we should anticipate that the dominant Franck-Condon factor will be for the final one-photon ionization step in which all vibrational quantum numbers are conserved (*i.e.* $\Delta v = 0$). This is nicely illustrated by the REMPI-PE spectra shown in Figures 5 and 6. The former, obtained following excitation of a *room temperature* NH_3 sample at (a) 286.84 nm ($2\tilde{\nu} = 69\,709$ cm^{-1}), (b) 279.20 nm ($2\tilde{\nu} = 71\,615$ cm^{-1}) and (c) 275.56 nm ($2\tilde{\nu} = 72\,560$ cm^{-1}), arise as a result of $2+1$ REMPI *via* the $1^1 2^3$, $1^1 2^5$ and $1^1 2^6$ vibronic levels of the $\tilde{C}'$ state, respectively. The $\tilde{C}'-\tilde{X}$ $1_0^1 2_0^3$, $1_0^1 2_0^5$ and $1_0^1 2_0^6$ bands appear only weakly in the parent two photon excitation spectrum, but are relatively free from overlap, and thus give "clean" photoelectron spectra (Fig. 5) each of which is dominated by a single peak appearing at a kinetic energy wholly consistent with an ionization step in which both the ν_1 and ν_2 quantum numbers are preserved. Lower members

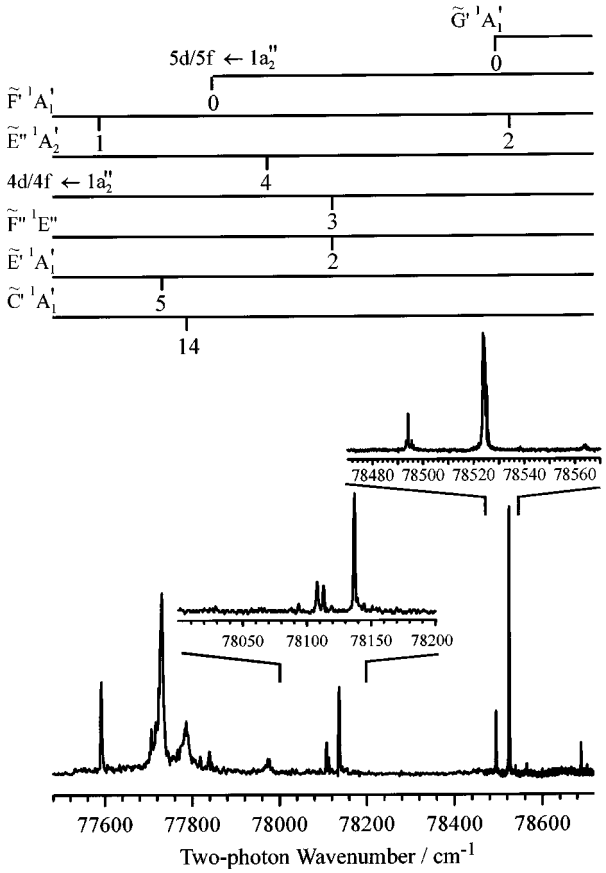

Fig. 4. $2+1$ REMPI spectrum of jet-cooled NH_3 recorded using linearly polarized laser radiation and monitoring just those ions with TOF appropriate to m/z 17, over the wavelength range 258.0–254.0 nm ($2\bar{\nu} = 77\,490$–$78\,720$ cm^{-1}). This spectrum is a composite, obtained by splicing together two spectra. Although some adjustments were made to avoid serious discontinuities between overlapping spectra, no corrections were made for variations in laser output energy. The numbers below the combs in the figure indicate v_2', the upper state out-of-plane bending quantum number. Relevant features for comparison with the REMPI-PE spectra presented in Figures 6 and 8 are shown on an expanded scale above the main spectrum.

of this $\tilde{C}'-\tilde{X}$ $1_0^1 2_0^n$ progression in NH_3 were identified in one of the first applications of REMPI-PES to NH_3 [31]. These spectra are included primarily to demonstrate the strong propensity for $\Delta v = 0$ transitions in the final one photon ionization step from the Rydberg states of ammonia, since it is an underlying assumption in much of our subsequent discussion. Figure 6 shows the corresponding REMPI-PES obtained following excitation at 254.72 nm ($2\tilde{\nu} = 78\,495$ cm^{-1}), resonant with one of the more prominent features apparent in the jet-cooled excitation spectrum shown in Figure 4. The fact that all REMPI-PE spectra reported herein were recorded using an effusive jet is significant in this case, because the room temperature band contour of this transition (and all other transitions) will be substantially wider than that shown in the jet-cooled excitation spectrum, and spectral overlap will

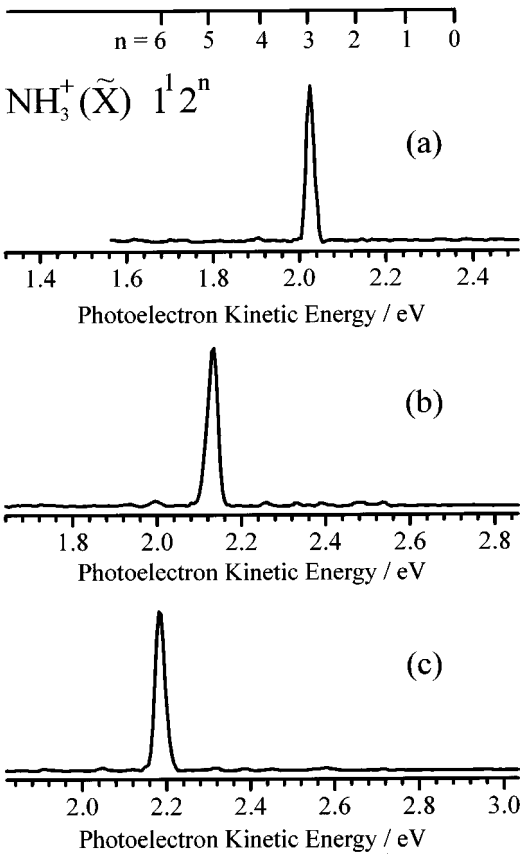

Fig. 5. REMPI-PE spectra of NH_3 obtained following excitation at (a) 286.84 nm ($2\tilde{\nu}$ = 69 709 cm^{-1}), (b) 279.20 nm ($2\tilde{\nu}$ = 71 615 cm^{-1}) and (c) 275.56 nm ($2\tilde{\nu}$ = 72 560 cm^{-1}). The three peaks at $KE = 2.03$, 2.13 and 2.19 eV, respectively, are consistent with NH_3^+ ion formation in the $1^1 2^3$, $1^1 2^5$ and $1^1 2^6$ vibrational states.

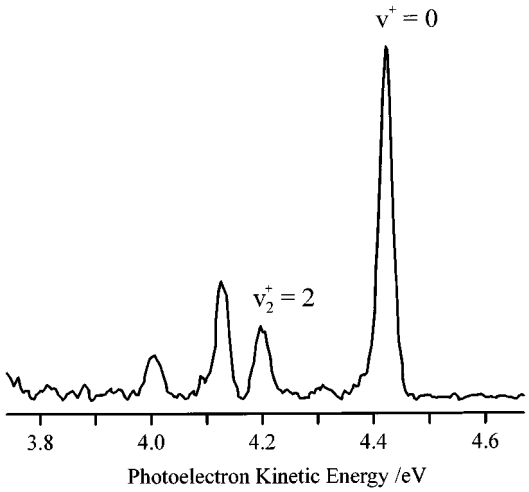

Fig. 6. REMPI-PE spectrum of NH_3 obtained following excitation at 254.72 nm ($2\tilde{\nu}$ = 78 495 cm^{-1}). The dominant peak, at $KE = 4.41$ eV, is consistent with ionization to the zero-point level of the ion, whilst that at $KE = 4.20$ eV is associated with ion formation in the $v_2^+ = 2$ level. The identity of the peak at $KE = 4.11$ eV is discussed in the text.

be correspondingly greater. The dominant peak appears with a $KE = 4.41$ eV. Energy conservation requires that

$$3h\nu = IE + E_{int}(NH_3^+) + KE(e^-). \quad (3)$$

Three 254.72 nm photons equate to a total energy of 14.60 eV. Thus, given the ionization threshold for forming NH_3^+ ($\tilde{X}$) ions, $IE = 10.19$ eV [33], we conclude that there is a strong propensity for forming parent ions with $E_{int} = 0.0$ eV, *i.e.* in their zero-point vibrational level. This suggests that the Rydberg level of NH_3 providing the dominant resonance enhancement at the two-photon energy following excitation at 254.72 nm is an electronic origin. This allows estimation of its quantum defect, δ, defined according to the relation

$$2\tilde{\nu} = IE - R/(n-\delta)^2, \quad (4)$$

where IE = 82 159 cm^{-1} and R is the Rydberg constant, 109 737 cm^{-1}. The value of δ reflects the extent to which the Rydberg electron penetrates into the core region and, as such, is a sensitive indicator of the ℓ character of the Rydberg electron. Such information, taken together with the results even of crude simulations of the corresponding band contours evident in the jet-cooled REMPI excitation spectra (which will often suffice to indicate the parallel or perpendicular nature of the two-photon excitation step), can be of considerable help in unravelling the vibronic level structure of small and medium size gas phase molecules at energies approaching the ionization limit. In this instance we deduce that the $2\tilde{\nu}$ = 78 495 cm^{-1} feature is the first (*i.e.* 0_0^0) member of a progression of parallel bands, the origin of which exhibits a quantum defect, $\delta = 0.53$ (assuming $n = 6$). This we assign in terms of the orbital promotion $6pa_2'' \leftarrow 1a_2''$, resulting in population of an excited state of $^1A_1'$ symmetry which has been labeled the $\tilde{G}'$ state [2].

The energy level diagram shown in Figure 7 anticipates results presented in Figure 8 by considering a situation where there are two levels (belonging to different Rydberg series both of which converge to the same electronic state of the ion (*e.g.* the ground state), with bending quantum numbers $v_2' = 2$ and 3, respectively, in near degeneracy. From the foregoing, it should be clear that one-photon ionization from these levels would result in preferential formation of NH_3^+ ($\tilde{X}$) ions with bending vibrational quantum numbers $v_2^+ = 2$ and 3, respectively. Obviously, these two states of the ion involve different amounts of internal (vibrational) energy but, since the particular intermediate levels of interest were near degenerate, the overall three-photon absorption will have introduced very similar amounts of energy in each case. Once again, energy conservation will be satisfied if the photoelectron is ejected with the appropriate kinetic energy (Eq. (3)). As before, knowing the total energy supplied to the molecule by the multiphoton absorption process, one can deduce the vibrational quantum state of the resulting ion and thus, by Franck-Condon arguments, the vibrational level(s) of the Rydberg state (or states) providing the resonance enhancement at the two-photon energy, simply by measuring the photoelectron KEs.

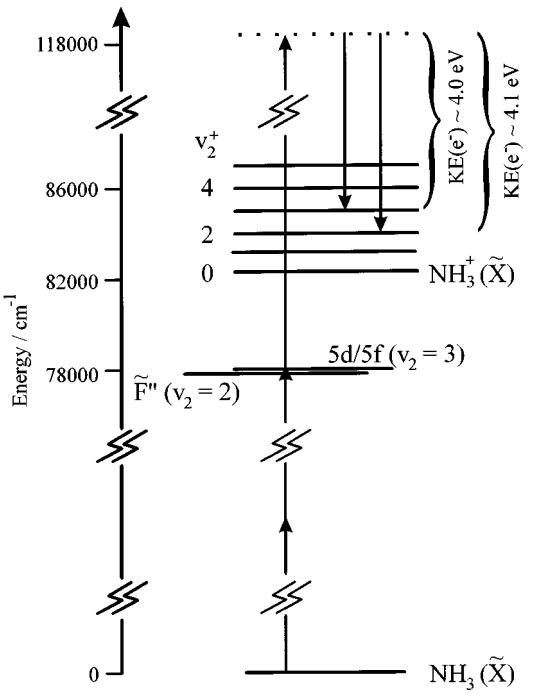

Fig. 7. Energy level diagram illustrating the origins of the various sub-groups in the photoelectron KE distribution that will result in the case of 2 + 1 REMPI *via* near degenerate Rydberg levels with bending vibrational quantum number $v_2' =$ 2 and 3, respectively (see text for further detail).

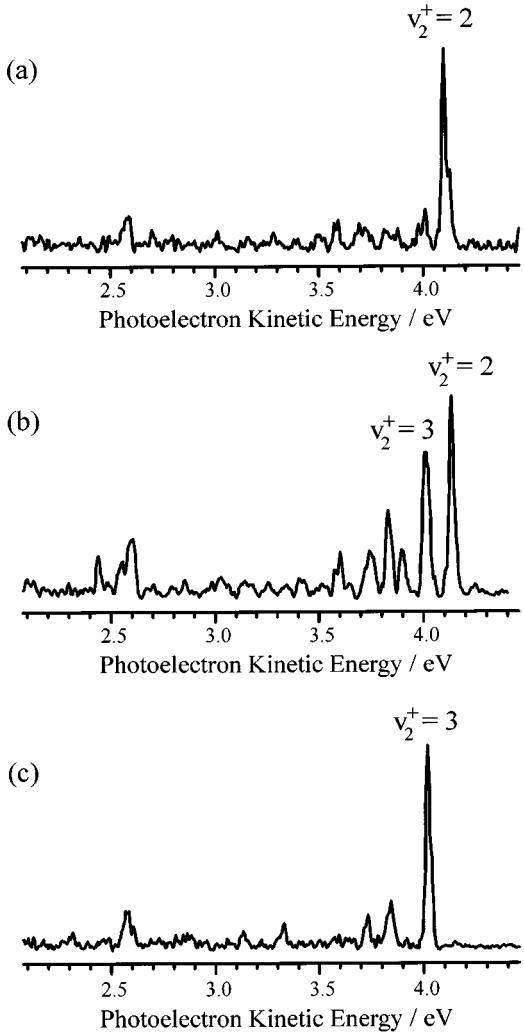

Fig. 8. REMPI-PE spectra of NH_3 obtained following excitation at (a) 256.09 nm ($2\tilde{\nu}$ = 78 074 cm^{-1}), (b) 255.87 nm ($2\tilde{\nu}$ = 78 142 cm^{-1}) and (c) 255.71 nm ($2\tilde{\nu}$ = 78 190 cm^{-1}). The strongest peak in (a), at $KE = 4.10$ eV, is consistent with ionization to the $v_2^+ = 2$ state of the ion, whilst that in (c), at $KE = 4.01$ eV, is consistent with formation of ions with $v_2^+ = 3$. The unlabeled weaker peaks in (a–c) can be assigned in terms of two photon resonance enhanced ionization *via* the $\tilde{E}''\ 2^4$, $\tilde{E}'\ 2^5$ and $\tilde{E}'\ 2^6$ states and *via* the $\tilde{E}'-\tilde{X}'\ 2_1^2 1_0^1$ "hot band", the band contours of each of which will overlap the relevant energy range when using a room temperature NH_3 sample.

Figure 8 shows three more REMPI-PE spectra, obtained following excitation of a room temperature NH_3 sample at (a) 256.09 nm ($2\tilde{\nu}$ = 78 074 cm^{-1}), (b) 255.87 nm ($2\tilde{\nu}$ = 78 142 cm^{-1}) and (c) 255.71 nm ($2\tilde{\nu}$ = 78 190 cm^{-1}). Note that the first and third of these REMPI-PE spectra were recorded at wavenumbers where the jet-cooled excitation spectrum (Fig. 4) shows no resonance enhancements. This, and the fact that the wavenumber used when recording (b) differs from that of the peak in the jet-cooled REMPI spectrum (Fig. 4), again is merely a reflection of the much broader vibronic band contours in the *room temperature* parent excitation spectrum. Consider the most intense peak with $KE = 4.10$ eV in (a). Three 256.09 nm photons correspond to a total energy of 14.52 eV. Given $IE(v^+ = 0) = 10.19$ eV [33], we this time deduce that there is a strong preference for forming parent ions with $E_{int} = 0.23$ eV – equivalent to 2 quanta of the out-of-plane bending vibration, v_2^+. Thus we conclude that the Rydberg level providing the two-photon resonance enhancement following excitation of room temperature NH_3 molecules at 256.09 nm also carries 2 quanta of out-of-plane bending vibration. Similar analysis of the REMPI-PE spectra obtained following excitation at 255.71 nm (c) indicates that the resulting ions are formed with $v_2^+ = 3$; hence the intermediate level assignments chosen in Figure 7 and indicated in the REMPI excitation spectrum shown in Figure 4. Excitation of a room temperature NH_3 sample at intermediate wavelengths (*e.g.* 255.87 nm) results in some resonance enhancement by the band contours of transitions to both of these intermediate levels, and a more complex REMPI-PE spectrum results (Fig. 8b).

Similar REMPI-PES measurements at neighbouring excitation wavelengths allow unambiguous identification of extended vibronic progressions associated with these peaks (and with the other resonance enhancements evident in Fig. 4) and, in each case, determination of the Rydberg state origin. This, in turn, allows estimation of the quantum defect, δ, of these various Rydberg origins. Thus, for example, we deduce that the two-photon resonance at $2\tilde{\nu} \sim 78\,140$ cm^{-1} involves contributions from the

third (*i.e.* 2_0^2) member of a progression of perpendicular bands the electronic origin of which lies at $\sim 76\,200$ cm^{-1} *and* with the fourth (*i.e.* 2_0^3) member of a second progression with electronic origin at $75\,335$ cm^{-1}. The δ values for these two origins are ~ 0.7 and ~ 0.0 (assuming $n = 5$ and $n = 4$ respectively). The former is associated with the orbital promotion $5pe' \leftarrow 1a_2''$, resulting in population of an excited state of $^1E''$ symmetry which has been labeled the F'' state [2]. Definitive assignment of the electronic state supporting the 2_0^3 band is more problematic; the near zero quantum defect suggests strongly that the terminating orbital is either a $4d$ or $4f$ Rydberg orbital.

Returning to Figure 6, the astute observer will have noted the presence of a number of weak features which we have not yet discussed, but which can be interpreted as arising from analogous, weaker, overlap of excited states of NH_3 resonant at the two photon energy. The peak at $KE = 4.20$ eV is consistent with $2 + 1$ REMPI terminating on the $v_2^+ = 2$ level of the ion [33]. Recalling the $2+1$ REMPI excitation spectrum shown in Figure 4, this is most readily explicable by assuming some two photon resonance enhancement by the nearby $\tilde{F}'^1A_1' - \tilde{X}\ 2_0^2$ band which, given that the REMPI-PES data was recorded using a *room temperature* sample, is perfectly feasible. More interesting is the feature at $KE = 4.11$ eV, with $E_{int} = 0.3$ eV (2420 cm^{-1}). This internal energy is no simple multiple of ν_2^+, but is most readily interpreted in terms of the formation of $NH_3^+(\tilde{X})$ ions carrying one quantum of each of ν_2^+ and ν_4^+ (ν_4 is the e' degenerate out-of-plane bending mode) [33]. Again, if we assume a $\Delta v = 0$ ionization step, such an assignment would suggest two-photon resonance enhancement by a $2_0^1 4_0^1$ band in the neutral NH_3 molecule which, on energetic grounds, we must associate with the $\tilde{F}''^1E''$ state with electronic origin at $\sim 76\,200$ cm^{-1} [2]. The vibronic symmetry of this $2^1 4^1$ level will be $^1E'' \otimes a_2'' \otimes e' = {}^1A_1'$. We attribute it's unexpected showing in the two photon excitation spectrum to accidental near resonance, and vibronic mixing, with the resonant $\tilde{G}'^1A_1'\ 0^0$ level. Such a $2_0^n 4_0^1$ transition is the analogue of those reported previously [24,27] involving the $\tilde{B}^1E''$ state, the first ($n = 3$) member of the $npe' \leftarrow 1a_2''$ Rydberg series to which the $\tilde{F}''$ state also belongs. Here, then, we see another example of a situation where careful analysis of REMPI-PES spectra can reveal contributions from vibronic mixing between excited state levels [38] which, by virtue of spectral overlap or their inherently weak transition strength, is not recognizable in the conventional wavelength resolved REMPI excitation spectrum.

4 Conclusions

This paper presents selected examples involving the molecules NH_3 and ND_3 which serve to demonstrate how a combination of (jet-cooled) REMPI spectroscopy and companion REMPI-PES studies can provide a wealth of detailed information relating to the energetic ordering of Rydberg states in small and medium sized gas phase molecules, even amongst the myriad of observed features converging on the first IE. It is not intended to provide a comprehensive guide to the current state of knowledge regarding the Rydberg states of ammonia – this can be found in references [2,7,8]. For a yet more detailed understanding of the dense manifold of highly excited states of ammonia it will almost certainly be necessary to take advantage of the additional spectral simplification and definition provided by two color double resonance spectroscopy methods.

The Bristol group acknowledges the technical advice and encouragement of Mr K.N. Rosser, and the EPSRC for equipment grants, postdoctoral support (SRL) and a Senior Research Fellowship (MNRA). AJO-E is grateful to the Royal Society for the award of the Eliz. Challenor Research Fellowship. The Amsterdam group acknowledges the Netherlands Organization for Scientific Research (NWO) for equipment grants and financial support and R.A. Rijkenberg for experimental assistance.

References

1. M.N.R. Ashfold, J.D. Howe, Ann. Rev. Phys. Chem. **45**, 57 (1994) and references therein.
2. S.R. Langford, A.J. Orr-Ewing, R.A. Morgan, C.M. Western, M.N.R. Ashfold, A. Rijkenberg, C.R. Scheper, W.J. Buma, C.A. de Lange, J. Chem. Phys. **108**, 6667 (1998).
3. A.E. Douglas, J.M. Hollas, Can. J. Phys. **39**, 479 (1961).
4. A.E. Douglas, Discuss. Faraday Soc. **35**, 158 (1963).
5. A.D. Walsh, P.A. Warsop, Trans. Faraday Soc. **57**, 345 (1961).
6. M.N.R. Ashfold, C.L. Bennett, R.J. Stickland, Comm. At. Mol. Phys. **19**, 181 (1987) and references therein.
7. G.C. Nieman, S.D. Colson, J. Chem. Phys. **68**, 5656 (1978); **71**, 571 (1979).
8. J.H. Glownia, S.J. Riley, S.D. Colson, G.C. Nieman, J. Chem. Phys. **72**, 5998 (1980); **73**, 4296 (1980).
9. L.D. Ziegler, J. Chem. Phys. **82**, 664 (1985).
10. M.N.R. Ashfold, C.L. Bennett, R.N. Dixon, Chem. Phys. **93**, 293 (1985); Faraday Discuss. Chem. Soc. **82**, 163 (1986).
11. J. Xie, G. Sha, X. Zhang, C. Zhang, Chem. Phys. Lett. **124**, 99 (1986).
12. S.A. Henck, M.A. Mason, W.B. Yan, K.K. Lehmann, S.L. Coy, J. Chem. Phys. **102**, 4783 (1995); **102**, 4772 (1995).
13. M.I. McCarthy, P. Rosmus, H-J. Werner, P. Botschwina, V. Vaida, J. Chem. Phys. **86**, 6693 (1987).
14. J. Biesner, L. Schnieder, J. Schmeer, G. Ahlers, X. Xie, K.H. Welge, M.N.R. Ashfold, R.N. Dixon, J. Chem. Phys. **88**, 3607 (1988); **91**, 2901 (1989).
15. M.N.R. Ashfold, R.N. Dixon, S.J. Irving, H-M. Koeppe, W. Meier, J.R. Nightingale, L. Schnieder, K.H. Welge, Philos. Trans. R. Soc. Lond. A **332**, 375 (1990).
16. D.H. Mordaunt, M.N.R. Ashfold, R.N. Dixon, J. Chem. Phys. **104**, 6460, 6472 (1996).
17. R.N. Dixon, Mol. Phys. **88**, 949 (1996).
18. M.N.R. Ashfold, D.H. Mordaunt, S.H.S. Wilson, in *Advances in Photochemistry*, edited by D.C. Neckers, D.H. Volman, G. von Bünau, Vol. 21 (Wiley, New York, 1996), p. 217.

19. M.N.R. Ashfold, R.N. Dixon, M. Kono, D.H. Mordaunt, C.L. Reed, Philos. Trans. R. Soc. Lond. A. **355**, 1659 (1997).
20. V. Vaida, W. Hess, J.L. Roebber, J. Phys. Chem. **88**, 3397 (1984).
21. X. Li, C.R. Vidal, J. Chem. Phys. **101**, 5523 (1994); **102**, 9167 (1995).
22. M.N.R. Ashfold, R.N. Dixon, R.J. Stickland, C.M. Western, Chem. Phys. Lett. **138**, 201 (1987).
23. M.N.R. Ashfold, R.N. Dixon, N. Little, R.J. Stickland, C.M. Western, J. Chem. Phys. **89**, 1754 (1988).
24. J.M. Allen, M.N.R. Ashfold, R.J. Stickland, C.M. Western, Mol. Phys. **74**, 49 (1991).
25. T. Seeleman, P. Andresen, E.W. Rothe, Chem. Phys. Lett. **146**, 89 (1988).
26. J.M. Allen, M.N.R. Ashfold, R.J. Stickland, C.M. Western, J. Chem. Soc. Faraday Trans. **86**, 2921 (1990).
27. J.M. Allen, M.N.R. Ashfold, C.L. Bennett, C.M. Western, Chem. Phys. Lett. **149**, 1 (1988).
28. X. Li, X. Xie, L. Li, X. Wang, C. Zhang, J. Chem. Phys. **97**, 128 (1992).
29. M.N.R. Ashfold, R.N. Dixon, R.J. Stickland, Chem. Phys. **88**, 463 (1984).
30. M.N.R. Ashfold, R.N. Dixon, K.N. Rosser, R.J. Stickland, C.M. Western, Chem. Phys. **101**, 467 (1986).
31. P.J. Miller, S.D. Colson, W.A. Chupka, Chem. Phys. Lett. **145**, 183 (1988).
32. M.R. Dobber, W.J. Buma, C.A. de Lange, J. Phys. Chem. **99**, 1671 (1995).
33. W. Habenicht, G. Reiser, K. Müller-Dethlefs, J. Chem. Phys. **95**, 4809 (1991); G. Reiser, W. Habenicht, K. Müller-Dethlefs, J. Chem. Phys. **98**, 8462 (1993).
34. M.N.R. Ashfold, C.M. Western, J.W. Hudgens, R.D. Johnson III, Chem. Phys. Lett. **260**, 27 (1996).
35. R.A. Morgan, A.J. Orr-Ewing, D. Ascenzi, M.N.R. Ashfold, W.J. Buma, C.R. Scheper, C.A. de Lange, J. Chem. Phys. **105**, 2141 (1996).
36. S. Urban, R. D'Cunha, K.N. Rao, D. Papousek, Can. J. Phys. **62**, 1775 (1984).
37. T.J. Slotterback, S.G. Clement, K.C. Janda, C.M. Western, J. Chem. Phys. **101**, 7221 (1994).
38. R.A. Morgan, A.J. Orr-Ewing, M.N.R. Ashfold, W.J. Buma, N.P.L. Wales, C.A. de Lange, J. Chem. Soc. Faraday Trans. **91**, 3339 (1995)
39. S. Urban, D. Papousek, M. Bester, K. Yamada, G. Winnewisser, A. Guarnieri, J. Mol. Spectrosc. **106**, 29 (1984).